Supplementary information

Table S1. Summary of the synthetic conditions

Sample	Reagents	Pressure, GPa	T, K	Products
1	NaN_3	50(3)*	1800(200)	Na_2N_5
2	$NaN_3 + N_2$	52(1)	2200 (200)	Na_2N_5 NaN_5 $NaN_5 \cdot N_2$
2	$NaN_3 + N_2$	34 (1)	< 1000	Na_3N_8
2	$NaN_3 + N_2$	14 (1)	< 1000	NaN_2

* non-hydrostatic conditions due to the absence of pressure-transmitting medium

Table S2

Crystal data				
Chemical formula	$NaN_5 \cdot N_2$	NaN_5	Na_3N_8	Na_2N_5
M_r	121.06	93.04	181.05	116.03
Crystal system, space group	Monoclinic, $P2_1/n$	Orthorhombic, $Pmn2_1$	Tetragonal, $I4_1/amd$	Monoclinic, Pm
Pressure (GPa)	52.9	52.9	32.4	50.0
a, b, c (Å)	10.321(3), 8.672 (3), 11.0409 (17)	5.455(6), 2.836(12), 5.662 (8)	4.8538(9), 16.037(10)	4.781 (10), 2.5873 (7), 4.934 (12)
β (°)	91.70 (2)			119.6 (3)
V (Å^3)	987.8 (5)	87.6 (4)	377.8 (3)	53.1 (2)
Z	16	2	4	1
Radiation type	Synchrotron, λ = 0.29521 Å			
μ (mm^{-1})	0.08	0.09	0.09	0.10
Data collection				
Diffractometer	13IDD @ APS			
Absorption correction	Multi-scan *CrysAlis PRO* 1.171.40.75a (Rigaku Oxford Diffraction, 2020)			
T_{min}, T_{max}	0.703, 1.000	0.465, 1.000	0.220, 1.000	0.598, 1.000
No. of measured, independent and observed [$I > 2\sigma(I)$] reflections	2419, 1474, 811	169, 133, 130	442, 164, 111	135, 115, 93
R_{int}	0.055	0.045	0.053	0.014
$(\sin\theta/\lambda)_{max}$ (Å^{-1})	0.894	0.887	0.859	0.853
Refinement				
$R[F^2 > 2\sigma(F^2)]$, $wR(F^2)$, S	0.079, 0.242, 0.99	0.053, 0.148, 1.24	0.040, 0.092, 0.98	0.057, 0.140, 1.11
No. of reflections	1474	133	164	115
No. of parameters	129	18	18	23
No. of restraints	8			2
$\Delta\rho_{max}$, $\Delta\rho_{min}$ (e Å^{-3})	0.70, −0.45	0.47, −0.60	0.32, −0.31	0.62, −0.40

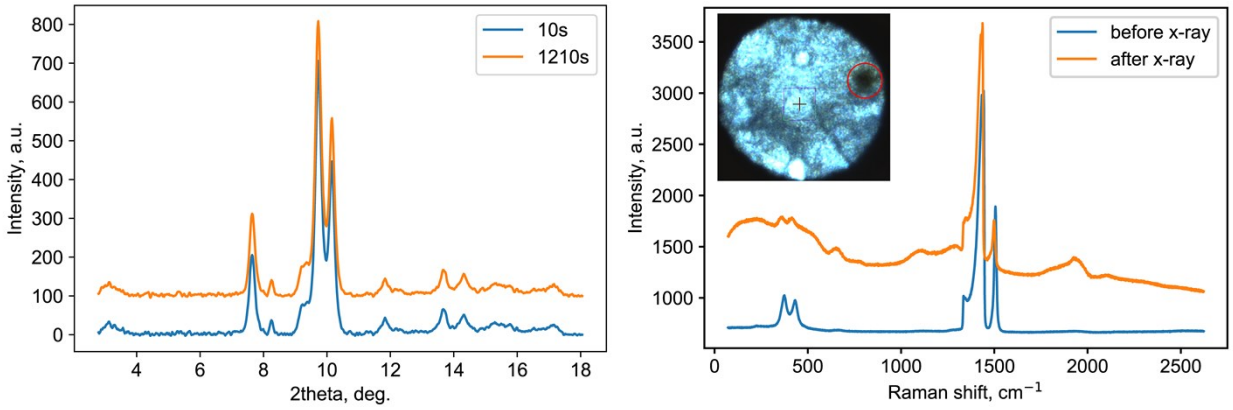

Figure S1. X-ray diffraction pattern of NaN_3 exposed to 37 keV X-ray radiation during 10 and 1210 s and corresponding Raman spectra. Raman spectrum of NaN_3 after X-ray exposure corresponds very well with the Raman spectrum of cold-compressed NaN_3 reported by Eremets et al. [1]. This phase was called NaN_3 phase II. The appearance of new bands around 1750-2000, 1100 and 1300 cm^{-1} suggests that new N-N bonds may form as a result of the interaction between N_3 units. However, no noticeable changes could be observed in the diffraction pattern, suggesting that the X-ray induced high-pressure phase of NaN_3 is amorphous in nature.

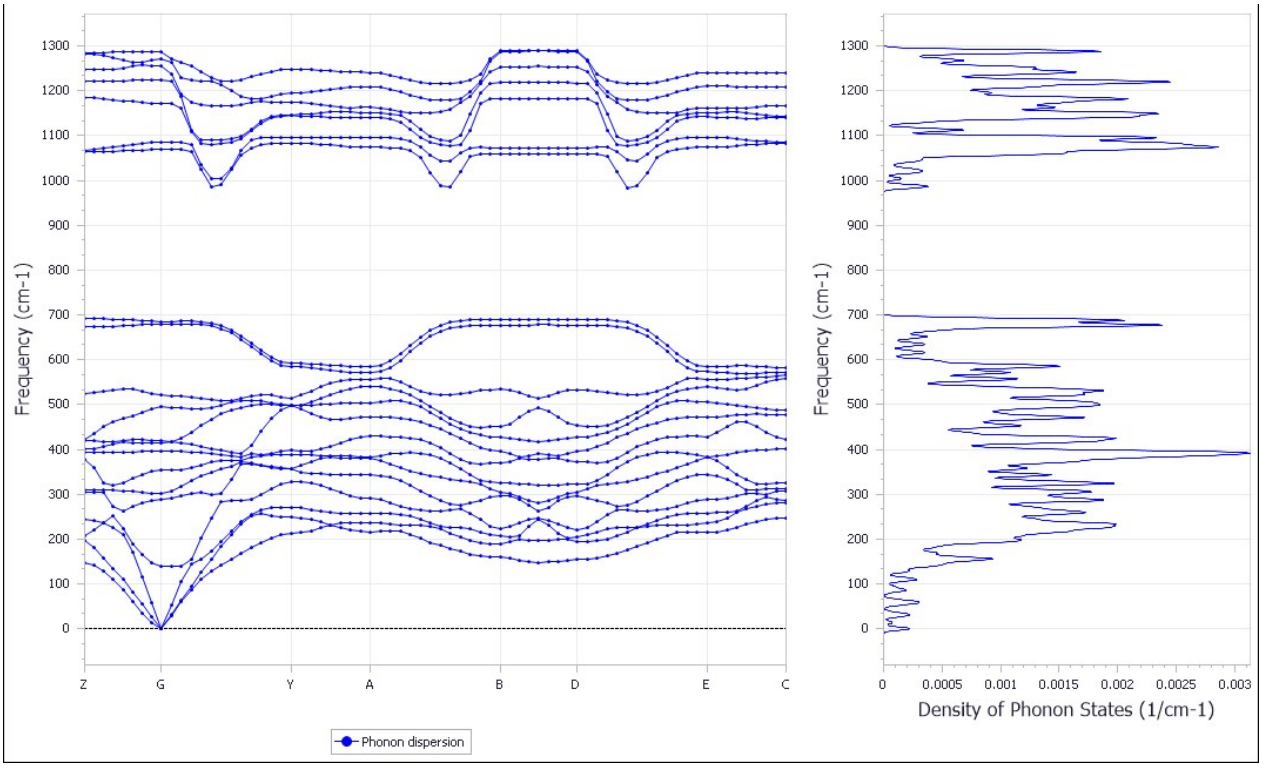

Figure S2. Calculated phonon dispersion curves and density of phonon states of Na_2N_5 at ~50 GPa.

Procedure for the analysis of the multigrain single-crystal X-ray diffraction dataset collected in a diamond anvil cell:

1. After the collection of a single-crystal X-ray diffraction dataset (series of ~120 frames, collected with a step of $\Delta\omega = 0.5°$) we perform a standard peak search procedure as implemented by *CryAlis*^{Pro} program.

2. We make a reconstruction of the peak search table in the reciprocal space (Figure S2a). The peak search table contains the peaks from all crystalline phases, which are present in the collection spot. These can be reaction products, initial reagents, pressure-transmitting medium, diamonds, gasket material, *etc*.

3. Inspecting the 3D reciprocal space (Figure S2a) in CryAlisPro, one finds reciprocal lattices of the well-diffracting phases (Figure S2b,c).

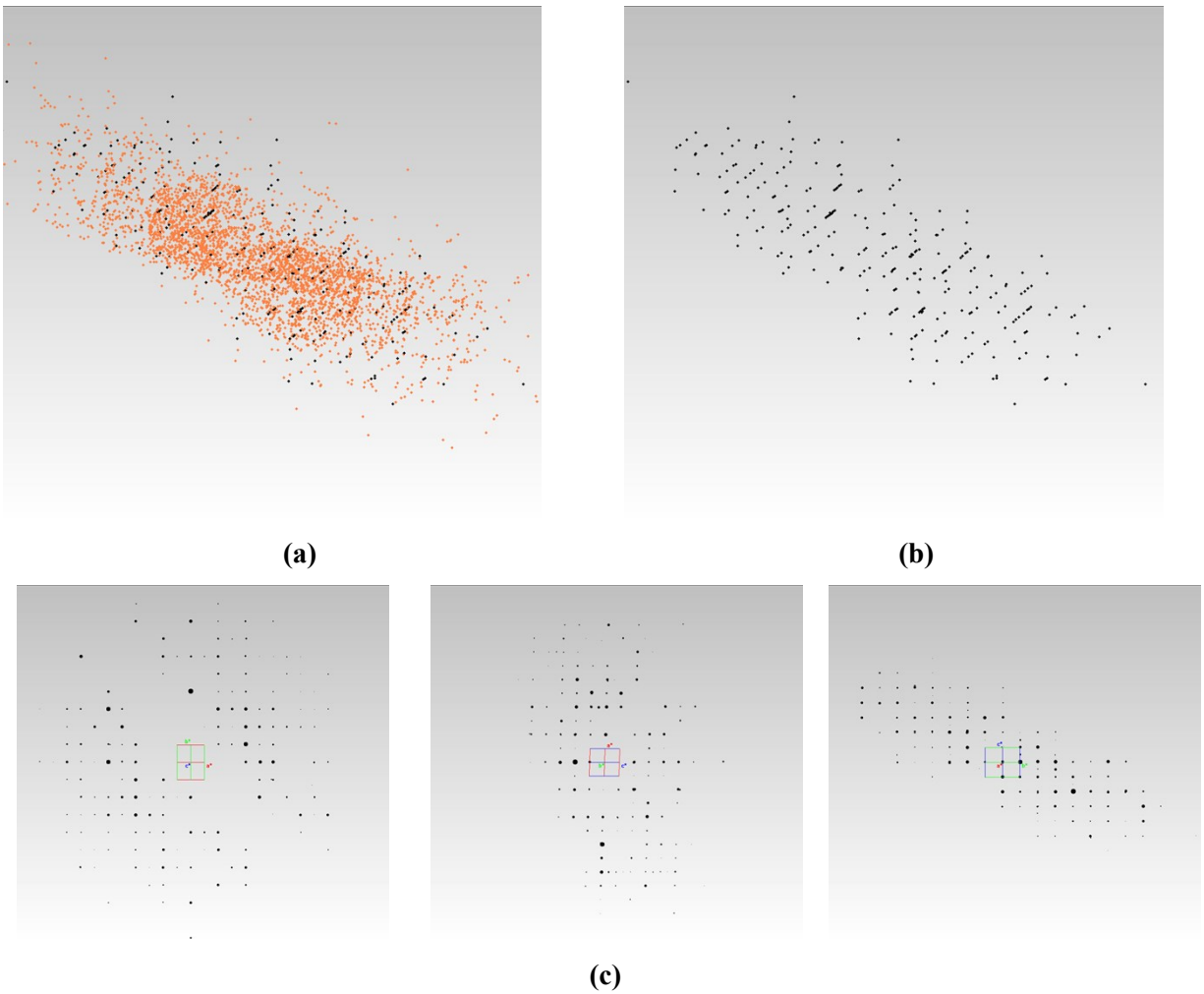

Figure S3. (a) The results of the peak search reconstruction in the reciprocal space. (b,c) The reciprocal lattice of NaN_7 extracted from (a).

4. The quality of indexing is then checked on the reconstructions of the reciprocal lattice planes. In the Figure S4a we show the reconstruction of the plane (*h*3*l*) as an example. First, we look if there are non-indexed peaks. In case they are present and form a regular pattern, it could mean that the found lattice parameters are incorrect (this is not the case in Figure S4a). Such a check is done for each accessible lattice plane. In our example, there are a few non-indexed peaks, which do not form a regular pattern. They may belong either to different grains of the same phase, or to different phases; this is clarified at the further steps of the analysis.

5. We perform the integration of the dataset using the orientation matrix for the found domain(s). The best indicator of the proper integration is a good value of Rint (5.5% in our dataset) and, of course, the possibility to solve and to refine the structure.

6. We try to find out if the lattice of the phase found first can describe all the reflections on the diffraction pattern. For that, we perform the 2D integration of the data to the "powder-like" Intensity vs 2Θ plot and make a Le-Bail fit (Figure S4c).

7. If we observe strong non-indexed peaks, we return to the step 3 in order to search for more phases.

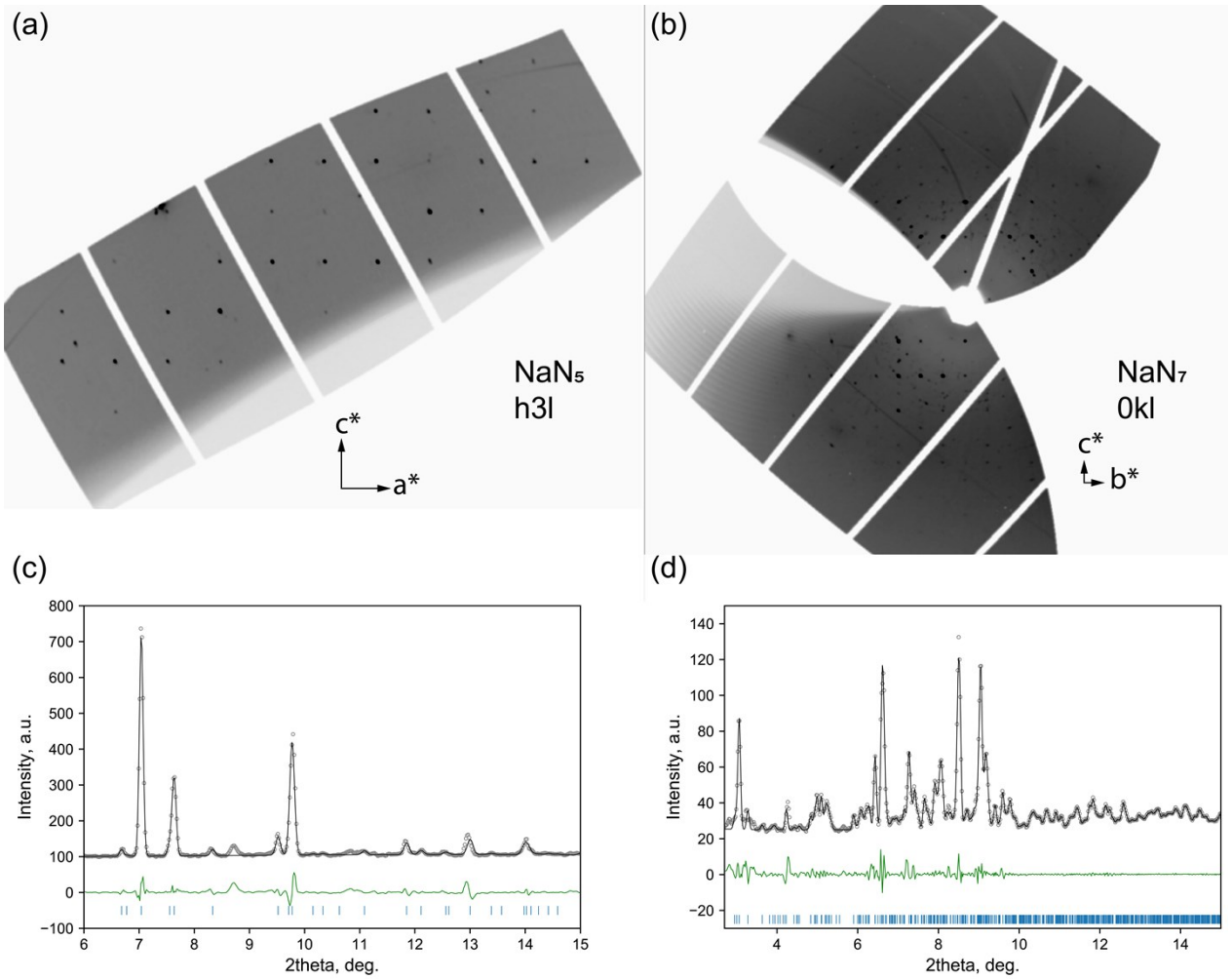

Figure S4. (a,b) Reconstruction of selected reciprocal lattice planes of NaN_5 and NaN_7. (c,d) Le-Bail fits of NaN_5 and NaN_7 at ~53 GPa respectively. Due to the large unit cell volume the peaks of NaN_7 severely overlap already at low angles but are clearly resolved in single-crystal XRD. The Le-Bail fit of NaN_7 is presented for demonstration purposes. Data extracted from this fit was not used in the paper.

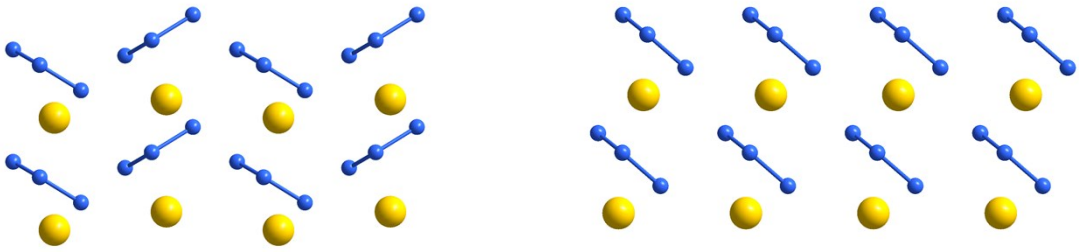

Figure S5. Comparison of experimental $Pmn2_1$ (left) and theoretical *Cm* [2] models of NaN_5 at ~50 GPa.

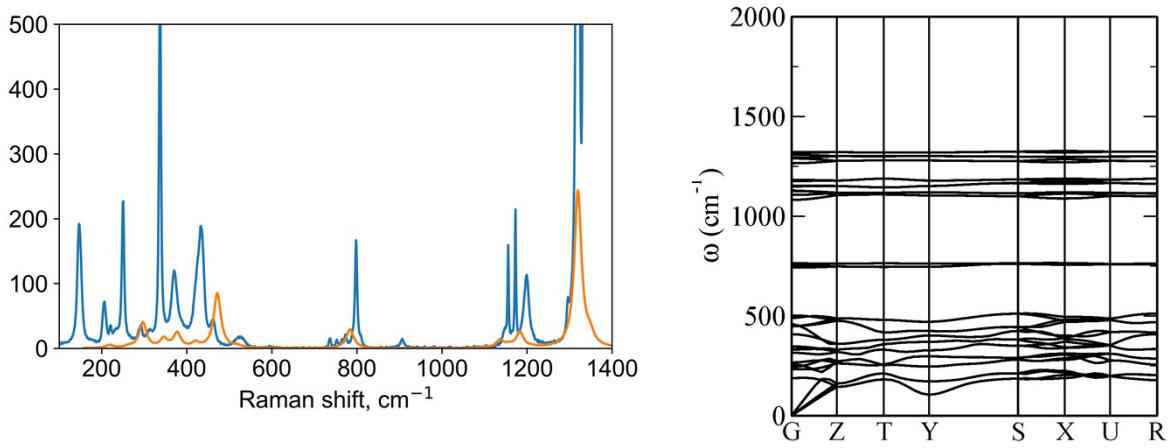

a **b**

Figure S6. (a) Calculated (orange) and experimental Raman spectra of NaN_5 at ~50 GPa. It is known that calculations may give frequencies, which slightly deviate from the experimental results. To "calibrate" the calculated Raman spectra we added 30 cm^{-1} shift to all the peaks. (b) Calculated phonon dispersions for NaN_5 at ~50 GPa.

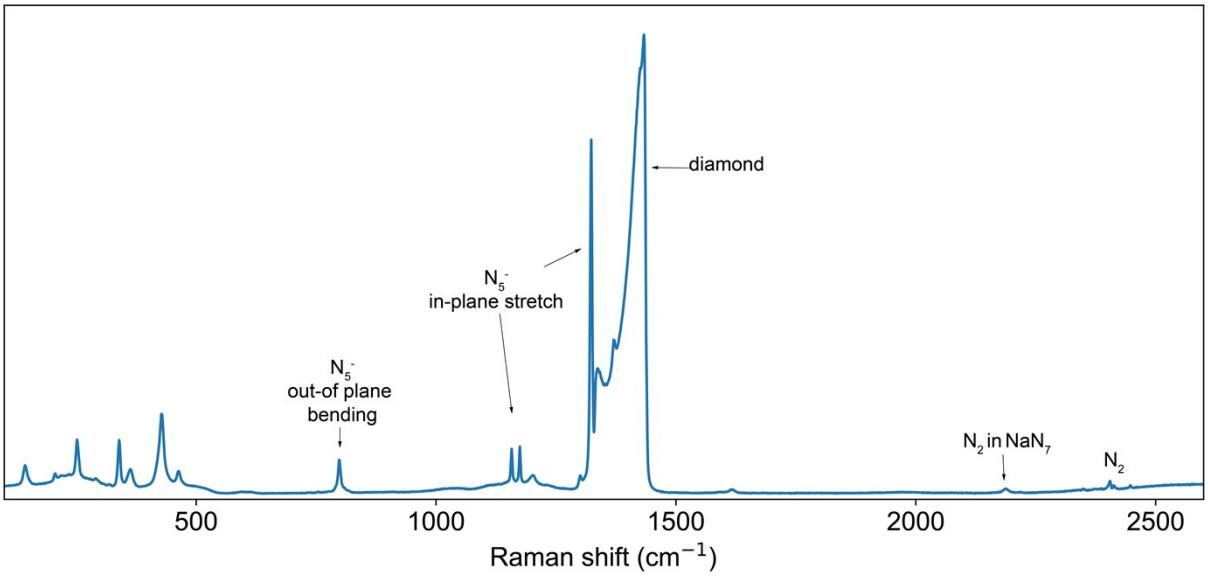

Figure S7. Raman spectra from a mixture of NaN_5 and NaN_7 phases at ~48 GPa.

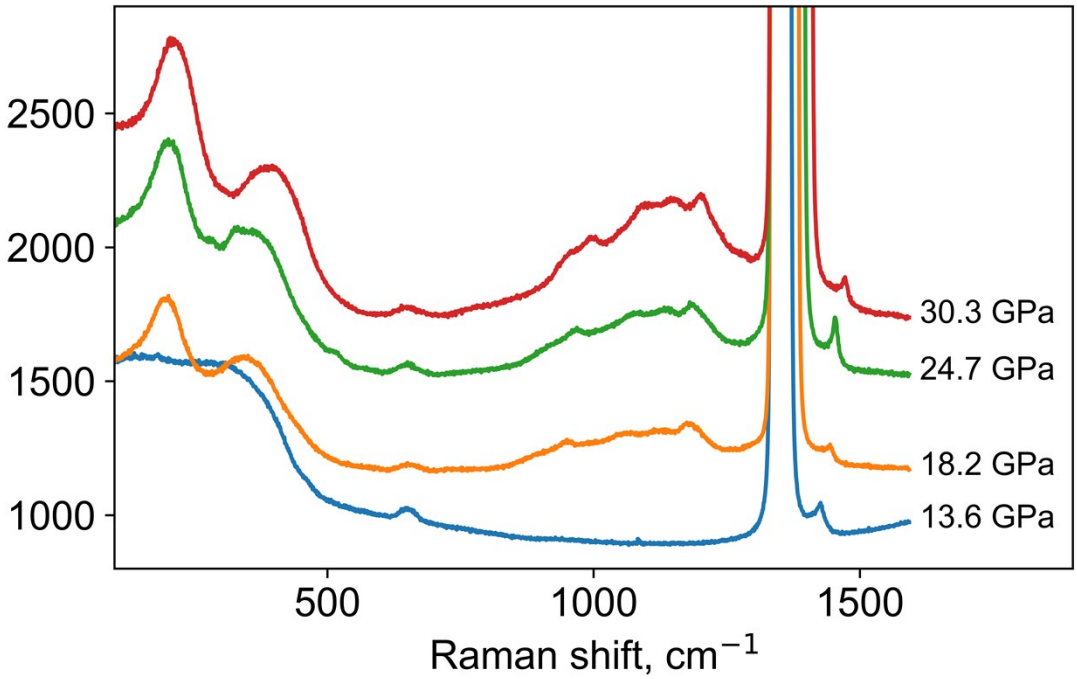

Figure S8. Raman spectra of Na_2N_5 on decompression.

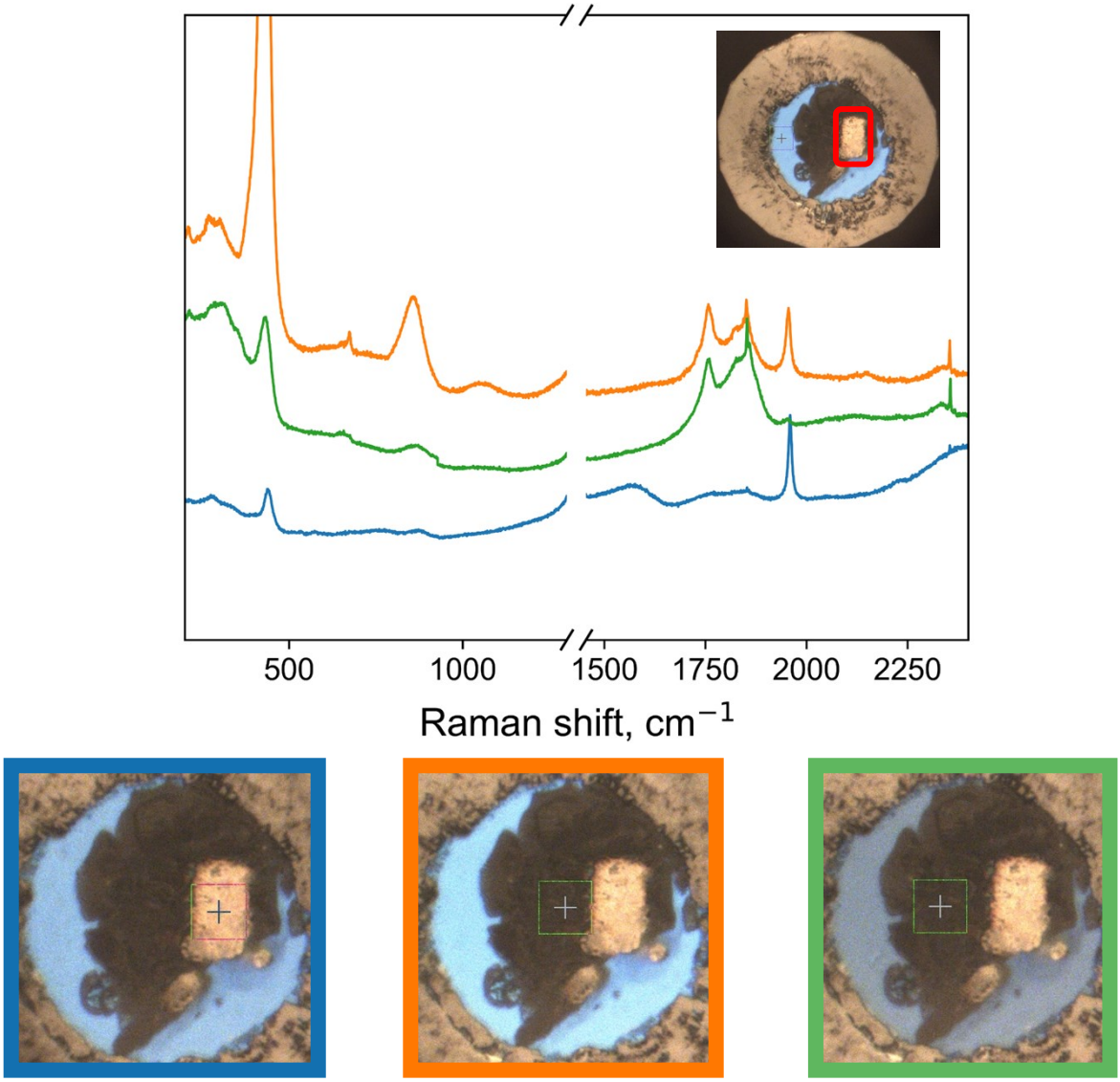

Figure S9. Raman spectra of the Sample #1 re-heated at ~14 GPa. heated area is highlighted in the inset of the upper figure. Raman spectra collection areas are marked by a cross on the microscopic images. The colors of the microscopic picture borders correspond to the colors of the Raman spectra. In the middle of the heated area (blue spectrum) there is a strong peak at ~ 1960 cm^{-1}, which gradually disappears when the data collection spot is moving out from the heated area (green spectrum).

References:

[1] M. I. Eremets, M. Y. Popov, et al., J. Chem. Phys. **120**, 10618 (2004) DOI:10.1063/1.1718250.

[2] B. A. Steele and I. I. Oleynik, Chem. Phys. Lett. **643**, 21 (2016) DOI:10.1016/j.cplett.2015.11.008.